

Geophysical Research Letters®



RESEARCH LETTER

10.1029/2023GL104121

Key Points:

- Branching angles of major stream networks on the eastern Tibetan Plateau vary systematically with climatic aridity and channel slopes
- Climatic controls dominate over tectonic drivers in shaping the branching angles in the flat interior of the eastern Tibetan Plateau
- Tectonic controls dominate over climate in shaping the branching angles in the steep margin of the eastern Tibetan Plateau

Supporting Information:

Supporting Information may be found in the online version of this article.

Correspondence to:


M. Li,
li-mh18@mails.tsinghua.edu.cn

Citation:

Li, M., Seybold, H., Wu, B., Chen, Y., & Kirchner, J. W. (2023). Interaction between tectonics and climate encoded in the planform geometry of stream networks on the eastern Tibetan Plateau. *Geophysical Research Letters*, 50, e2023GL104121. <https://doi.org/10.1029/2023GL104121>

Received 13 APR 2023
Accepted 23 JUN 2023

Interaction Between Tectonics and Climate Encoded in the Planform Geometry of Stream Networks on the Eastern Tibetan Plateau

Minhui Li^{1,2,3} , Hansjörg Seybold³ , Baosheng Wu^{1,2} , Yi Chen^{1,2}, and James W. Kirchner^{3,4,5} 

¹State Key Laboratory of Hydrosphere Science and Engineering, Department of Hydraulic Engineering, Tsinghua University, Beijing, China, ²Key Laboratory of Hydrosphere Sciences of the Ministry of Water Resources, Tsinghua University, Beijing, China, ³Department of Environmental Systems Science, ETH Zurich, Zurich, Switzerland, ⁴Swiss Federal Research Institute WSL, Birmensdorf, Switzerland, ⁵Department of Earth and Planetary Science, University of California, Berkeley, CA, USA

Abstract Stream networks are highly abundant across Earth's surface, reflecting the tectonic and climatic history under which they have developed. Recent studies suggest that branching angles are strongly correlated with climatic aridity. However, the impact of tectonic forcing, especially in tectonically active regions, remains ambiguous. Here we analyze branching angles between headwater channels of the major river networks on the eastern Tibetan Plateau, a region with complex tectonics, variable climate, and diverse landscapes. We find that spatial variations in tectonic uplift (as reflected in channel gradients) shape the branching geometry of stream networks on the steep eastern margin, while in the flat interior of the eastern Tibetan Plateau, branching angles are mainly controlled by climatic aridity. This leads to the conclusion that, in the steep margin of the eastern Tibetan Plateau, climatic impacts on branching angles are overprinted by stronger tectonic controls.

Plain Language Summary The geometry of stream networks reflects the tectonic and climatic evolution of landscapes. Prior studies show that stream branching angles tend to be wider in wetter climates. However, branching angles are also shaped by topography and thus by tectonic forcing, and the importance of climate relative to tectonics is unclear. Here we analyze branching angles formed between pairs of headwater channels of major river networks on the eastern Tibetan Plateau, where climatic aridity and channel slopes vary systematically from the relatively flat, dry interior to the steep, wet margin. The results show that stream network branching angles reflect the joint influence of tectonic forcing and climate. In the flat interior, branching angles are wider in wetter climates, consistent with previous studies in other regions. However, in the steep eastern margin, branching angles become narrower as climate becomes wetter and topographic gradients simultaneously become steeper. These results indicate that climatic controls on branching angles are gradually overwhelmed by tectonic controls as one goes from the relatively flat terrain of the interior to the steeper terrain of the tectonically active eastern margin.

1. Introduction

Numerous studies suggest that Earth's topography is shaped by the interplay between climate and tectonic forcing (Whittaker, 2012). River systems, for example, adjust their planform and profile geometry in response to erosion and uplift, and thus record information about a landscape's evolutionary past (Kwang et al., 2021; Perron et al., 2012; Seybold et al., 2021). Exploring the drivers that control the morphology of river systems can therefore provide insights into the processes that have shaped Earth's surface.

The branching angle formed by two incoming tributaries is a key morphological attribute that characterizes the planform geometry of stream networks. Thus, it may be diagnostic for the erosion processes at play and reveal how these processes vary across different tectonic and climatic zones. Recent studies have shown that mean branching angles are strongly related to climatic aridity not only across the United States (Getrauer & Maloof, 2021; Seybold et al., 2017) but also globally (Seybold et al., 2018; Strong & Mudd, 2022). Branching angles are typically narrower in arid regions than in humid climates, suggesting differences in the dominant erosion mechanisms (Seybold et al., 2017). In arid climates, headward growth of stream networks is more dominated by overland flow erosion (Horton, 1945). Overland flow occurs when rainfall exceeds soil infiltration capacity and thus the water is routed downhill along the line of steepest descent (Horton, 1945), leading to narrower branching angles. In humid climates, where infiltration rates are higher (Berghuijs et al., 2022) diffusive processes such as soil creep

© 2023. The Authors.

This is an open access article under the terms of the [Creative Commons Attribution License](https://creativecommons.org/licenses/by/4.0/), which permits use, distribution and reproduction in any medium, provided the original work is properly cited.

or groundwater flow are more common and valley heads tend to bifurcate at wider angles close to the characteristic angle of diffusive growth $\alpha = 2\pi/5 = 72^\circ$ (Carleson & Makarov, 2002; Devauchelle et al., 2012; Petroff et al., 2013). As a result the network's optimal configuration also varies with climate (Strong & Mudd, 2022). Branching angles are not only formed by headward growth of two incipient tributaries, but also by side branches which split off a larger stream. Such side branches are usually smaller creeks that enter a larger stream from the surrounding hillslopes, and thus generally have much steeper slopes and smaller drainage areas than the main channel that runs along the valley bottom. These differences in slope and upstream drainage area are also reflected in wider branching angles, often close to 90° (Getraer & Maloof, 2021; Horton, 1945; Strong & Mudd, 2022).

Erosional processes are influenced by both climatic and tectonic forcing (Hurst et al., 2019; Whittaker, 2012), and it has been widely recognized that gradients in precipitation control spatial variations in erosion rates in regions with relatively uniform tectonically driven rock uplift rates (Ferrier et al., 2013; Henck et al., 2011; Reiners et al., 2003). In contrast, uplift and hillslope processes become major drivers of erosion rates in tectonically active margins (Harkins et al., 2007; Vance et al., 2003), potentially leading to different drainage patterns for debris-flow dominated channels compared to fluvially dominated ones when the drainage area is 1 km^2 or less (Hooshyar et al., 2017; Stock & Dietrich, 2003). Surface slope is closely related to gradients in tectonic uplift and therefore plays an important role in shaping river basins. Steeper slopes tend to develop narrower and lengthier basins, with correspondingly narrower branching angles, because of less flow convergence (Castelltort et al., 2009; Castelltort & Yamato, 2013; Jung et al., 2011; Seybold et al., 2017).

To better understand the interplay between tectonic forcing and climate in shaping a stream network's geometry, here we analyze the morphology of the river systems of the eastern Tibetan Plateau. The Tibetan Plateau is a particularly interesting study area due to its strong gradients in climate and surface uplift (Clark et al., 2004). The Tibetan Plateau, often referred to as the Third Pole (Qiu, 2008), was formed primarily by the collision and continued convergence between the Indian and Eurasian plates (Wu et al., 2019), and its eastward growth is thought to be driven by crustal shortening or viscous lower crustal flow (Royden et al., 2008; Tapponnier et al., 2001). The growth of the Himalayas and the Tibetan Plateau accounts for the large-scale drainage patterns of most Asian river systems (Chen et al., 2021; Clark et al., 2004; Li et al., 2022; Yang et al., 2015) which encompass a wide range of landscapes in different climatic and tectonic zones. With an average elevation of more than 4,000 m above sea level, the Tibetan Plateau acts as a barrier for westerlies and monsoon circulation (Zhao et al., 2022). These topographic conditions create strong climatic gradients between the plateau's arid interior and its monsoon-influenced southeast margin (Hudson & Quade, 2013). The increase in precipitation from the flat interior to the highly dissected eastern margin is generally accompanied by topographic steepening.

Unraveling the link between river network geometry and geomorphological processes on the Tibetan Plateau is challenging due to strong coupling and feedbacks between climate and uplifted topography, which also characterize many of the world's major mountain belts. While our study focuses on the formation of stream network branching angles under the joint influence of climate and tectonic forcing on the eastern Tibetan Plateau, our results may also provide general clues for the development of stream networks in tectonically active regions.

2. Data and Methods

2.1. Stream Networks and Branching Angles

The Tibetan Plateau, known as the water tower of Asia, is the source of most of Asia's largest rivers (Immerzeel et al., 2010). Our study focuses on the river systems of the eastern Tibetan Plateau, including the Yellow, Yangtze, Mekong and Salween Rivers, as well as the Yarlung (Tsangpo) River downstream of its confluence with the Lasa River (Figure 1).

The stream networks analyzed in this study have been extracted from the 90-m-resolution Shuttle Radar Topography Mission Digital Elevation Model (SRTM-DEM) (<http://srtm.csi.cgiar.org>) using the code DEMRiver (Bai et al., 2015). For the network extraction, we set the critical source area threshold to 100 pixels, corresponding to roughly $\sim 1 \text{ km}^2$. An overlay of our extracted stream network superimposed on aerial imagery (Figure S1 in Supporting Information S1) indicates that the extraction technique produces good results even in flat terrain.

We calculated branching angles (α) between upstream tributaries following the approach described by Seybold et al. (2017), which includes the following three steps. First, we converted the stream networks' segments with

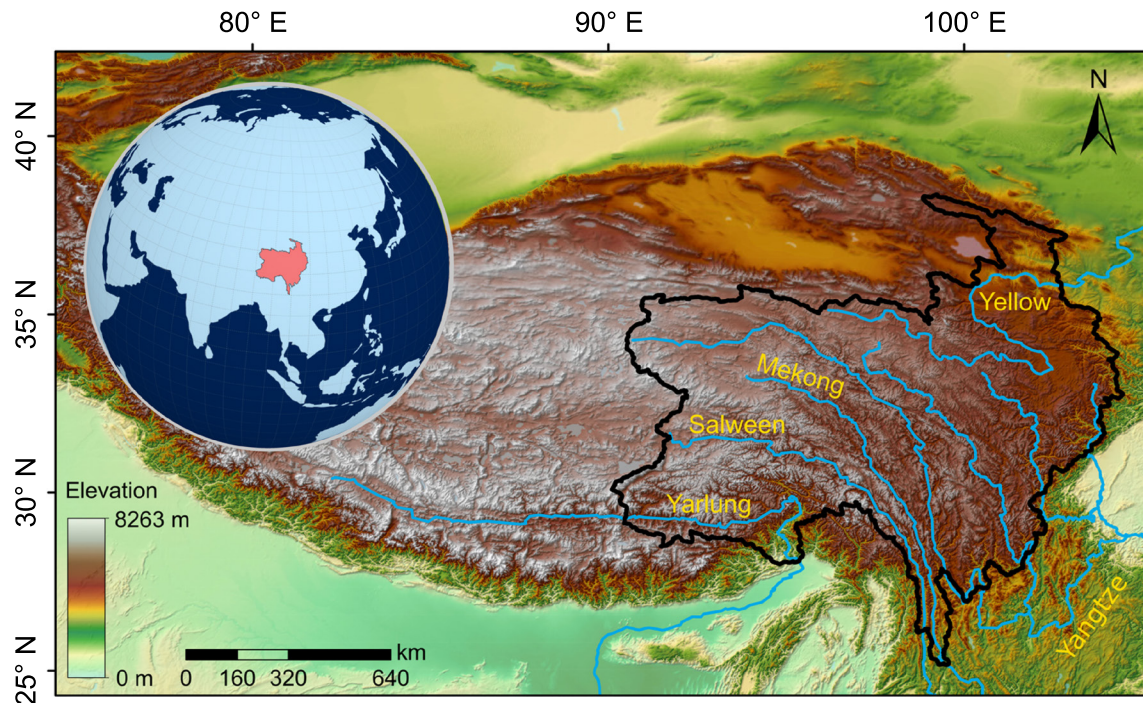


Figure 1. Context map of the Tibetan Plateau showing topography and major rivers (blue lines) in our study area, the boundary of which is denoted by a solid black line. The inset shows the location of the study area on the globe.

a conformal projection (Lambert conformal conic) into a series of points ordered from upstream to downstream. In the next step, we fit straight lines to the points comprising the two upstream tributaries (mean length 1.63 ± 1.19 km) using orthogonal least squares. Finally, we calculated the angle between the orientations of the two regression lines.

To rule out complex interdependencies between branching angles and network connectivity, our analysis is restricted to the comparison of branching angles formed by pairs of first-order headwater channels; these are termed first-order branching angles in the remainder of the manuscript. Using headwater channel pairs with comparable drainage areas and slopes largely eliminates the influence of differences in drainage area and slope ratios on branching angles. Doing so also mitigates the impact of network concavity, which inherently regulates slope ratios (Getraer & Maloof, 2021; Strong & Mudd, 2022). Although flow regimes, whether dominated by debris flow or fluvial processes, exhibit distinct characteristic angles (Hooshyar et al., 2017), no transition in flow regime is observed in the slope-area curve of our data set (Figure S2 in Supporting Information S1).

Junctions formed by tributaries with fewer than 3 pixels (shorter than 270 m) were omitted from analysis to avoid systematic artifacts due to the limited number of points available for determining the direction of the channel segment using orthogonal regression. We also excluded junctions formed by channels with slopes of less than 0.0001 because flow routing across low-gradient landscapes often produces unreliable channel locations (Strong & Mudd, 2022).

To explore the spatial variability of branching angles across the Tibetan Plateau and minimize any artifacts resulting from variations in junction densities (Text S1, Table S2, and Figures S5–S7 in Supporting Information S1), we average our first-order branching angles (α) and the channel slopes (S_c) of their upstream tributaries within hexagons of area $A = 2,500$ km². This approach yields 403 hexagons containing on average 78 first-order branching angles per hexagon.

2.2. Climatic and Tectonic Metrics

The Aridity Index ($AI = P/PET$) is often used to describe climatic conditions because it represents the balance between precipitation (P) and the evaporative demand of the atmosphere, as quantified by potential evaporation

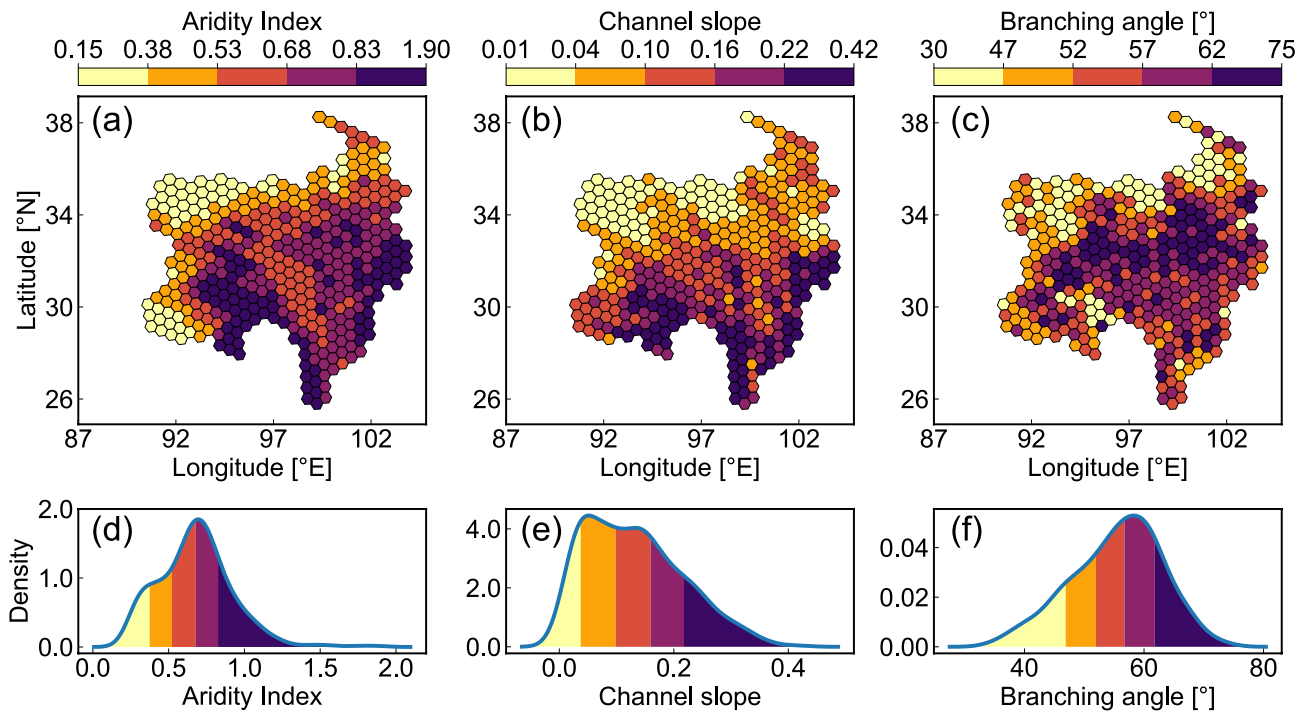


Figure 2. Spatial variability of hexagon-averaged (a) aridity index (AI), (b) first-order headwater channel slopes (S_c) and (c) first-order branching angles (α) across our study area. AI and S_c generally increase from northwest to southeast, reflecting more humid climates and steeper landscapes in the southeast. Branching angles in the headwater reaches of the major rivers are usually narrower than in the other parts. Panels (d–f) show the corresponding kernel density distributions for AI, S_c , and α .

(PET). For our analysis of the eastern Tibetan Plateau, we calculate the mean AI value in each hexagon using the aridity data from the Global Aridity and PET Database (Trabucco & Zomer, 2018). Note that because AI is defined as the ratio of precipitation to potential evapotranspiration, higher values of AI mean more humid conditions.

Tectonic forcing can create topography and maintain relief through surface uplift. Widely used topographic metrics to characterize tectonic activity are mean hillslope gradients, local relief, and channel steepness (Whipple, 2004). Topographic slopes have been widely used as proxies of erosional response to spatial variations in tectonic uplift rates (Kirby & Whipple, 2012; Seybold et al., 2021; Whipple, 2004). Hillslope gradients are often used to characterize surface roughness but cease to provide a proxy for erosion at high rates (>0.2 mm/a) because they reach the threshold of hillslope stability (Ouimet et al., 2009). By contrast, channel slopes can be more reliable erosion proxies in rapidly eroding landscapes, because they continue to steepen with increasing erosion rates. Therefore, first-order channel slope (S_c) is used in correlation analyses to quantify the impact of tectonic activity on stream networks' mean branching angles.

3. Results and Discussion

3.1. Spatial Patterns in Branching Angles, Climate and Tectonics

Figures 2a–2c shows the spatial variability of aridity index (AI), first-order headwater channel slope (S_c), and first-order branching angles (α) averaged over each 2,500 km² hexagon across the eastern Tibetan Plateau, together with their kernel density distributions in Figures 2d and 2e. Regional patterns are clearly visible, with AI values varying between 0.16 in the dry northwestern part of our study area and 1.87 at the most humid southeastern plateau margin (Figure 2a). Here, the deep valleys cut by the Yarlung and Salween Rivers serve as moisture paths for the South Asian Monsoon (Chen et al., 2021).

Except for the poorly drained low-relief areas of the Ruergai Basin near the first bend of the Yellow River, first-order headwater channel slopes tend to increase from the northwest ($S_c < 0.04$) to the southeast ($S_c > 0.22$) (Figure 2b), with a mean value of $S_c \sim 0.13$ across the whole Tibetan Plateau. On the steep southeastern margin

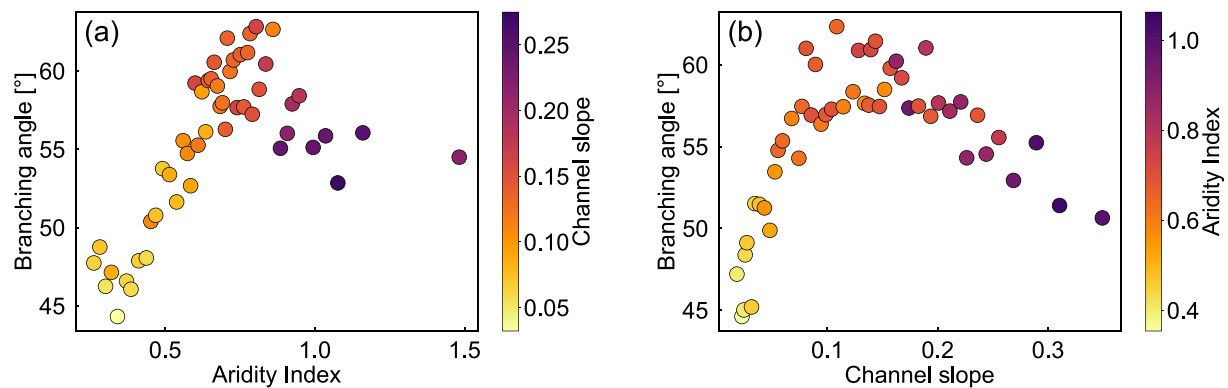


Figure 3. Variations in mean first-order branching angles with (a) aridity index AI and (b) channel slope (S_c). Each point contains $\sim 2\%$ of the whole data. The color gradient in (a) shows the variation of the average channel slope S_c , and in (b) it shows the variation in AI from dry (light colors) to humid (dark colors). Branching angles increase with increasing AI up to $AI \approx 0.75$ and decrease as AI increases further, but points with high AI also have high S_c . A similar pattern is found in the relationship between branching angle and channel slopes: branching angles first increase with increasing S_c (as AI increases), and then decrease with increasing S_c (while AI remains high). The interdependence of channel slope and AI is shown in Figure S3 in Supporting Information S1.

of the Tibetan Plateau, Asia's big rivers have carved deep valleys into the uplifting bedrock. Deeply incised gorges and very steep rivers often coexist in zones of rapid rock uplift and incision (Hodges et al., 2001; Wang et al., 2014). In the Tsangpo Gorge, for example, the channel drops by almost ~ 2 km in a stretch of less than ~ 50 km (Wang et al., 2014).

Hexagon-averaged first-order branching angles in the flat and dry interior tend to be systematically narrower than in other regions of the study area. Additionally, the widest branching angles tend to occur in the middle of our study area, where the interior meets the eastern margin of the Plateau (Figure 2c). Going further toward the southeastern foot of the Tibetan Plateau, branching angles tend to become narrower although the climate becomes more humid (AI increases). The strong tectonic forcing near the margin generally leads to steeper channels which converge at narrower angle because runoff has a greater slope-parallel component due to the gravitational forces acting on the flow (Castelltort et al., 2009; Castelltort & Yamato, 2013; Seybold et al., 2017). This suggests that branching angles on the eastern Tibetan Plateau may be the result of climatic signals superimposed on tectonic drivers.

To explore the interdependence of branching angles, climatic aridity (here quantified by the aridity index AI), and tectonic forcing (here proxied by channel slope S_c), we first analyzed how first-order branching angles vary with AI alone (Figure 3a). In our figure we sorted the hexagons based on their averaged AI and then binned the data by equal frequency. Each bin contains $\sim 2\%$ of the hexagons and is colored by the average slope of first-order channels analyzed in our data set. Average branching angles increase systematically with increasing humidity (AI values of up to ≈ 0.75), and then start to decrease as AI increases further. From Figure 3a we see that these humid (high-AI) hexagons also tend to have steep channel slopes, reflecting their proximity to the steep southeast margin of the Tibetan Plateau. A similar pattern is seen in the relationship between branching angles and channel slopes (Figure 3b), where again each point represents the binned mean of 2% of the hexagons, and is colored to reflect the average AI in each bin. In Figure 3b, mean branching angles first increase with increasing channel slopes (as AI increases, reflecting increasing humidity), then decrease with increasing channel slopes (as AI remains high near the southeast margin of the Plateau). Similar relationships were found with channel steepness index instead of channel slope (Text S2 and Figure S8 in Supporting Information S1). These observations lead to the hypothesis that strong differences in topographic uplift caused by the collision of the Indian and Eurasian plates are a significant driver of the planform geometry of stream networks in the wet and steep southeastern margin of the Tibetan Plateau.

3.2. Climatic and Tectonic Controls on Branching Angles

To disentangle the influence of climate and tectonic forcing, we divided our data set into 2 geographically distinct zones with roughly equal area, namely the northwest (blue) and the southeast (red) with 204 and 199 hexagons respectively (Figure 4a). The northwestern zone dry (mean AI = 0.42) and relatively flat (mean channel

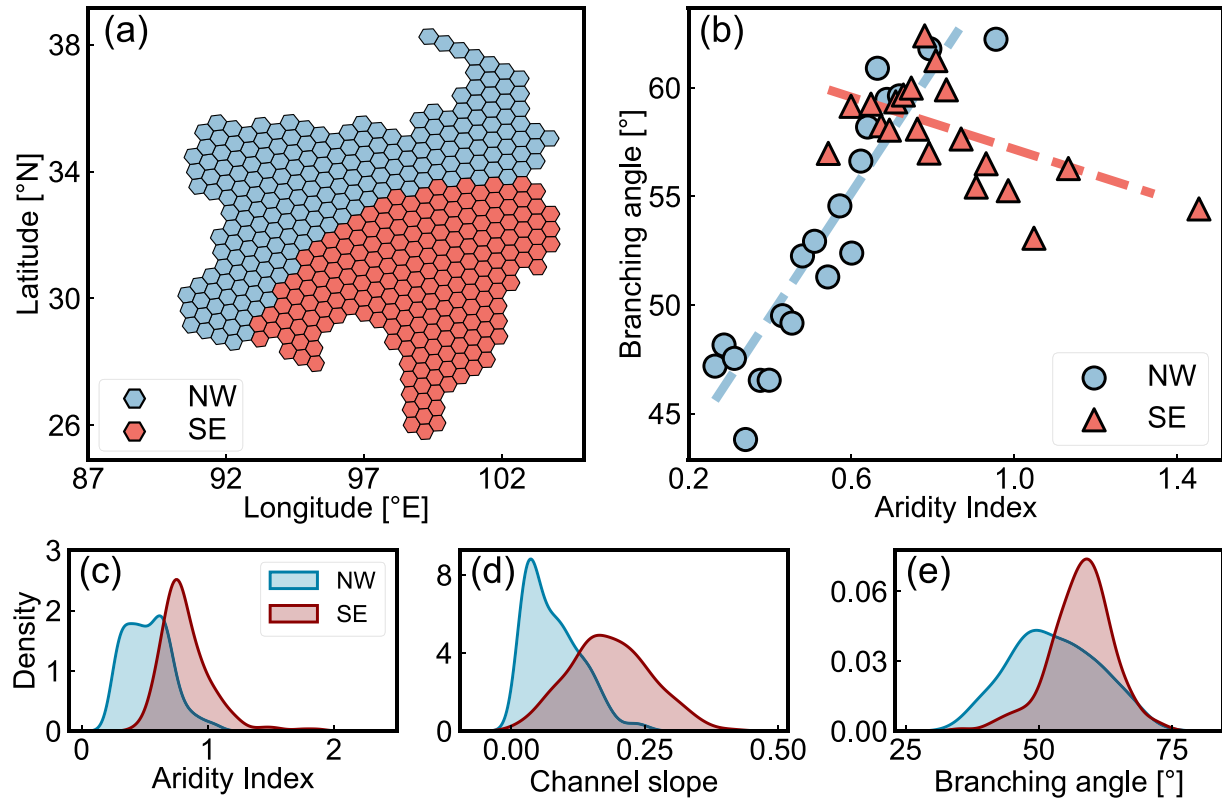


Figure 4. (a) Spatial distribution of the northwestern interior (NW) and southeastern margin (SE). (b) Relationships between the hexagon-averaged α and AI in the northwestern interior and southeastern margin. Each bin contains $\sim 5\%$ of the separate data set. (c–e) Kernel density estimate plots of aridity index, channel slope and branching angle. For the hexagons (blue) located in the flat interior of our study, α systematically increases with AI, while the hexagons (red), found primarily along the steep southeastern margin of the plateau, show a systematic decrease of α with AI.

slope = 0.08), primarily encompassing the headwater regions of the Yellow, Yangtze, Mekong, and Salween rivers. On the other hand, the southeastern margin of the plateau is humid (mean AI = 0.83) and steep (mean channel slope = 0.19). The kernel density distributions of AI, channel slope and branching angles in these two zones are shown in Figures 4c–4e respectively. Branching angles systematically increase with AI (Spearman $\rho = 0.65$, $p < 0.01$, Figure 4b) in the flat interior in the northwest of our study area. By contrast, hexagon-averaged branching angles in the steep southeastern margin systematically decrease with AI (Spearman $\rho = -0.19$, $p < 0.01$) and show a strong negative correlation with channel gradient (Spearman $\rho = -0.50$, $p < 0.01$, Table S1 in Supporting Information S1). These results suggest that the effect of channel slope on branching angles overprints climatic controls in this steep and tectonically active zone in the southeast of the Tibetan Plateau.

The relative impact of AI and channel slope (S_c) on branching angles (α) can also be described by a multiple regression model,

$$\alpha = \beta_0 + \beta_1 AI + \beta_2 S_c + \beta_3 (AI \cdot S_c) \quad (1)$$

where the branching angle α is approximated as a linear function of AI, S_c , and their interaction (denoted by $AI \cdot S_c$). Here, β_i indicate the regression coefficients. Applying Equation 1 with Z-scores for all the variables quantifies the normalized importance of AI and S_c , allowing us to compare their relative impact on α between the flat interior and the steep margin.

For the whole data set, we find that AI and channel slopes are strongly interdependent (Spearman $\rho = 0.62$, $p < 0.01$), and thus their interaction term has a strong effect on the overall relationship between branching angles and climatic (AI) and tectonic (S_c) influences. Across our whole study area, AI and channel slope account for roughly 40% of the observed variance in hexagon-averaged first-order branching angles (Table 1). While AI and channel slopes are positively correlated with branching angles, the regression coefficient of their interaction

Table 1
Multiple Regression Parameters for the Whole Eastern Tibetan Plateau Data Set (ETP), the Northwestern Zone (NW) and the Southeastern Zone (SE)

	ETP	NW	SE
AI	0.49	0.60	−0.08
S_c	0.04	0.24	−0.44
$AI \cdot S_c$	−0.49	−0.14	−0.03
R-squared	0.40	0.48	0.23

Note. All variables were converted to Z-scores. Regression parameters with $p < 0.01$ are shown in bold.

term is strongly negative, and this interaction effect may reverse the apparent correlation that one sees when branching angles are plotted as functions of AI or channel slope alone. AI has the strongest control on hexagon-averaged first-order branching angles ($\beta = 0.60$, $p < 0.01$) in the flat interior (i.e., the northwest hexagons) but does not significantly influence branching angles near the steep southeastern margin ($\beta = -0.08$, $p > 0.2$). Conversely, in the steep zone in the southeast (red hexagons in Figure 4a), channel slope is the dominant factor ($\beta = -0.44$, $p < 0.01$) in controlling the networks' branching angles and thus overprints the positive relationship between branching angles and AI. Steep slopes enhance the slope-parallel component of gravitational forces, leading to less flow convergence and therefore narrower branching angles. The interaction effect between AI and channel slopes is weaker (and thus the effects of AI and channel slopes are more clearly expressed) when flat northwestern zone (blue) and the steep southeastern zone (red) are considered separately (Table 1). These results are not very sensitive with

respect to the particular division of the Tibetan Plateau in the northwest (blue) and southeast (red) (Figure S4 in Supporting Information S1).

4. Conclusions

In this study, we evaluated the relative dominance of climatic aridity and channel slope in shaping the branching angles of stream networks on the eastern Tibetan Plateau. Our analysis shows that spatial patterns in average first-order branching angles reflect spatial gradients in climatic aridity and channel slope. On the eastern Tibetan Plateau, the correlation between first-order branching angles and climatic aridity reverses between the relatively flat interior and the steep eastern margin. In the flat interior, branching angles primarily reflect variations in climatic aridity, consistent with prior studies. Going from the flat interior to the steep margin, tectonic forcing becomes increasingly important as a control on branching angle variability, leading to an inverse correlation between branching angles and climatic aridity. These findings demonstrate the joint influence of tectonic forcing and climate in shaping river network morphology.

Data Availability Statement

The hexagon-averaged dataset used to produce our results is accessible under https://figshare.com/articles/dataset/Branching_angle_hexagon_ETP/23501547.

Acknowledgments

This study was partly supported by the Fund Program of State Key Laboratory of Hydrosience and Engineering (2023-KY-02) and National Natural Science Foundation of China (No. U2243218). Minhui Li acknowledges support from the Chinese Scholarship Council (202106210152).

References

- Bai, R., Li, T. J., Huang, Y. F., Li, J. Y., & Wang, G. Q. (2015). An efficient and comprehensive method for drainage network extraction from DEM with billions of pixels using a size-balanced binary search tree. *Geomorphology*, 238, 56–67. <https://doi.org/10.1016/j.geomorph.2015.02.028>
- Berghuijs, W. R., Luijendijk, E., Moeck, C., van der Velde, Y., & Allen, S. T. (2022). Global recharge data set indicates strengthened groundwater connection to surface fluxes. *Geophysical Research Letters*, 49(23), e2022GL099010. <https://doi.org/10.1029/2022gl099010>
- Carleson, L., & Makarov, N. (2002). Laplacian path models. *Journal d'Analyse Mathématique*, 87(1), 103–150. <https://doi.org/10.1007/bf02868471>
- Castelltort, S., Simpson, G., & Darriulat, A. (2009). Slope-control on the aspect ratio of river basins. *Terra Nova*, 21(4), 265–270. <https://doi.org/10.1111/j.1365-3121.2009.00880.x>
- Castelltort, S., & Yamato, P. (2013). The influence of surface slope on the shape of river basins: Comparison between nature and numerical landscape simulations. *Geomorphology*, 192, 71–79. <https://doi.org/10.1016/j.geomorph.2013.03.022>
- Chen, Y., Wu, B., Xiong, Z., Zan, J., Zhang, B., Zhang, R., et al. (2021). Evolution of eastern Tibetan river systems is driven by the indentation of India. *Communications Earth & Environment*, 2(1), 1–7. <https://doi.org/10.1038/s43247-021-00330-4>
- Clark, M. K., Schoenbohm, L. M., Royden, L. H., Whipple, K. X., Burchfiel, B. C., Zhang, X., et al. (2004). Surface uplift, tectonics, and erosion of eastern Tibet from large-scale drainage patterns. *Tectonics*, 23(1), TC1006. <https://doi.org/10.1029/2002tc001402>
- Devauchelle, O., Petroff, A. P., Seybold, H. J., & Rothman, D. H. (2012). Ramification of stream networks. *Proceedings of the National Academy of Sciences of the United States of America*, 109(51), 20832–20836. <https://doi.org/10.1073/pnas.1215218109>
- Ferrier, K. L., Huppert, K. L., & Perron, J. T. (2013). Climatic control of bedrock river incision. *Nature*, 496(7444), 206–209. <https://doi.org/10.1038/nature11982>
- Getrauer, A., & Maloof, A. C. (2021). Climate-driven variability in runoff erosion encoded in stream network geometry. *Geophysical Research Letters*, 48(3), e2020GL091777. <https://doi.org/10.1029/2020gl091777>
- Harkins, N., Kirby, E., Heimsath, A., Robinson, R., & Reiser, U. (2007). Transient fluvial incision in the headwaters of the Yellow River, north-eastern Tibet, China. *Journal of Geophysical Research*, 112(F3), F03S04. <https://doi.org/10.1029/2006j000570>

- Henck, A. C., Huntington, K. W., Stone, J. O., Montgomery, D. R., & Hallet, B. (2011). Spatial controls on erosion in the Three Rivers Region, southeastern Tibet and southwestern China. *Earth and Planetary Science Letters*, 303(1–2), 71–83. <https://doi.org/10.1016/j.epsl.2010.12.038>
- Hodges, K. V., Hurtado, J. M., & Whipple, K. X. (2001). Southward extrusion of Tibetan crust and its effect on Himalayan tectonics. *Tectonics*, 20(6), 799–809. <https://doi.org/10.1029/2001tc001281>
- Hooshyar, M., Singh, A., & Wang, D. (2017). Hydrologic controls on junction angle of river networks. *Water Resources Research*, 53(5), 4073–4083. <https://doi.org/10.1002/2016wr020267>
- Horton, R. E. (1945). Erosional development of streams and their drainage basins - Hydrophysical approach to quantitative morphology. *Geological Society of America Bulletin*, 56(3), 275–370. [https://doi.org/10.1130/0016-7606\(1945\)56\[275:edosat\]2.0.co;2](https://doi.org/10.1130/0016-7606(1945)56[275:edosat]2.0.co;2)
- Hudson, A. M., & Quade, J. (2013). Long-term east-west asymmetry in monsoon rainfall on the Tibetan Plateau. *Geology*, 41(3), 351–354. <https://doi.org/10.1130/g33837.1>
- Hurst, M. D., Grieve, S. W. D., Clubb, F. J., & Mudd, S. M. (2019). Detection of channel-hillslope coupling along a tectonic gradient. *Earth and Planetary Science Letters*, 522, 30–39. <https://doi.org/10.1016/j.epsl.2019.06.018>
- Immerzeel, W. W., Van Beek, L. P. H., & Bierkens, M. F. P. (2010). Climate change will affect the Asian water towers. *Science*, 328(5984), 1382–1385. <https://doi.org/10.1126/science.1183188>
- Jung, K. C., Niemann, J. D., & Huang, X. J. (2011). Under what conditions do parallel river networks occur? *Geomorphology*, 132(3–4), 260–271. <https://doi.org/10.1016/j.geomorph.2011.05.014>
- Kirby, E., & Whipple, K. X. (2012). Expression of active tectonics in erosional landscapes. *Journal of Structural Geology*, 44, 54–75. <https://doi.org/10.1016/j.jsg.2012.07.009>
- Kwang, J. S., Langston, A. L., & Parker, G. (2021). The role of lateral erosion in the evolution of nondendritic drainage networks to dendricity and the persistence of dynamic networks. *Proceedings of the National Academy of Sciences of the United States of America*, 118(16), e2015770118. <https://doi.org/10.1073/pnas.2015770118>
- Li, M. H., Wu, B. S., Chen, Y., & Li, D. (2022). Quantification of river network types based on hierarchical structures. *Catena*, 211, 105986. <https://doi.org/10.1016/j.catena.2021.105986>
- Ouimet, W. B., Whipple, K. X., & Granger, D. E. (2009). Beyond threshold hillslopes: Channel adjustment to base-level fall in tectonically active mountain ranges. *Geology*, 37(7), 579–582. <https://doi.org/10.1130/g30013a.1>
- Perron, J. T., Richardson, P. W., Ferrier, K. L., & Lapotre, M. (2012). The root of branching river networks. *Nature*, 492(7427), 100–103. <https://doi.org/10.1038/nature11672>
- Petroff, A. P., Devauchelle, O., Seybold, H., & Rothman, D. H. (2013). Bifurcation dynamics of natural drainage networks. *Philosophical Transactions of the Royal Society A: Mathematical, Physical & Engineering Sciences*, 371(2004), 20120365. <https://doi.org/10.1098/rsta.2012.0365>
- Qiu, J. (2008). China: The third pole. *Nature*, 454(7203), 393–396. <https://doi.org/10.1038/454393a>
- Reiners, P. W., Ehlers, T. A., Mitchell, S. G., & Montgomery, D. R. (2003). Coupled spatial variations in precipitation and long-term erosion rates across the Washington Cascades. *Nature*, 426(6967), 645–647. <https://doi.org/10.1038/nature02111>
- Royden, L. H., Burchfiel, B. C., & van der Hilst, R. D. (2008). The geological evolution of the Tibetan Plateau. *Science*, 321(5892), 1054–1058. <https://doi.org/10.1126/science.1155371>
- Seybold, H. J., Berghuijs, W. R., Prancevic, J. P., & Kirchner, J. W. (2021). Global dominance of tectonics over climate in shaping river longitudinal profiles. *Nature Geoscience*, 14(7), 503–507. <https://doi.org/10.1038/s41561-021-00720-5>
- Seybold, H. J., Kite, E., & Kirchner, J. W. (2018). Branching geometry of valley networks on Mars and Earth and its implications for early Martian climate. *Science Advances*, 4(6), eaar6692. <https://doi.org/10.1126/sciadv.aar6692>
- Seybold, H. J., Rothman, D. H., & Kirchner, J. W. (2017). Climate's watermark in the geometry of stream networks. *Geophysical Research Letters*, 44(5), 2272–2280. <https://doi.org/10.1002/2016gl072089>
- Stock, J., & Dietrich, W. E. (2003). Valley incision by debris flows: Evidence of a topographic signature. *Water Resources Research*, 39(4), 1089. <https://doi.org/10.1029/2001wr001057>
- Strong, C. M., & Mudd, S. M. (2022). Explaining the climate sensitivity of junction geometry in global river networks. *Proceedings of the National Academy of Sciences*, 119(50), e2211942119. <https://doi.org/10.1073/pnas.2211942119>
- Tapponnier, P., Xu, Z. Q., Roger, F., Meyer, B., Arnaud, N., Wittlinger, G., & Yang, J. S. (2001). Geology - Oblique stepwise rise and growth of the Tibet Plateau. *Science*, 294(5547), 1671–1677. <https://doi.org/10.1126/science.105978>
- Trabucco, A., & Zomer, R. J. (2018). Global aridity index and potential evapotranspiration (ET0) climate database v2. *CGIAR Consortium Spatial Information*, 10, m9.
- Vance, D., Bickle, M., Ivy-Ochs, S., & Kubik, P. W. (2003). Erosion and exhumation in the Himalaya from cosmogenic isotope inventories of river sediments. *Earth and Planetary Science Letters*, 206(3–4), 273–288. [https://doi.org/10.1016/s0012-821x\(02\)01102-0](https://doi.org/10.1016/s0012-821x(02)01102-0)
- Wang, P., Scherler, D., Liu-Zeng, J., Mey, J., Avouac, J. P., Zhang, Y. D., & Shi, D. G. (2014). Tectonic control of Yarlung Tsangpo Gorge revealed by a buried canyon in Southern Tibet. *Science*, 346(6212), 978–981. <https://doi.org/10.1126/science.1259041>
- Whipple, K. X. (2004). Bedrock rivers and the geomorphology of active orogens. *Annual Review of Earth and Planetary Sciences*, 32(1), 151–185. <https://doi.org/10.1146/annurev.earth.32.101802.120356>
- Whittaker, A. C. (2012). How do landscapes record tectonics and climate? *Lithosphere*, 4(2), 160–164. <https://doi.org/10.1130/rlf.1003.1>
- Wu, C., Zuza, A. V., Zhou, Z. G., Yin, A., McRivette, M. W., Chen, X. H., et al. (2019). Mesozoic-Cenozoic evolution of the Eastern Kunlun Range, central Tibet, and implications for basin evolution during the Indo-Asian collision. *Lithosphere*, 11(4), 524–550. <https://doi.org/10.1130/l11065.1>
- Yang, R., Willett, S. D., & Goren, L. (2015). In situ low-relief landscape formation as a result of river network disruption. *Nature*, 520(7548), 526–529. <https://doi.org/10.1038/nature14354>
- Zhao, R., Fu, P., Zhou, Y., Xiao, X. M., Grebbly, S., Zhang, G. Q., & Dong, J. (2022). Annual 30-m big lake maps of the Tibetan Plateau in 1991–2018. *Scientific Data*, 9(1), 164. <https://doi.org/10.1038/s41597-022-01275-9>